Granular Matter (2019) 21:89
https://doi.org/10.1007/s10035-019-0948-9

ORIGINAL PAPER

Capturing transient granular rheology with extended fabric tensor relations

Eduardo Rojas Parra[1] · **Ken Kamrin**[2]

Received: 3 March 2019

Abstract
We present an improved continuum model for transient processes in granular simple shearing, which predicts the coupled evolution of the effective friction coefficient and fabric tensor. Specifically, the model gives the transient strength associated to the kinematics and the structure of the granular media for the quasi-static regime. The results of the continuum model were compared against molecular dynamic simulations. The comparison for the modulus and the angle of the principal directions of the fabric tensor showed a very good agreement for all the cases analyzed. The new fabric evolution model is capable of capturing the abrupt fall in the fabric modulus and in the effective friction coefficient at the beginning of reversal processes, when the network is destroyed. The model also predicts the right spin direction of the fabric angle, when the force chains move from one steady state to another, during reversal. Improvement in modeling the stress is obtained by relating the friction coefficient to the fabric and the unit shear rate tensors.

Keywords Granular materials · Transient rheology · Fabric tensor · Effective friction coefficient

1 Introduction

Dense granular flows are the focus of enormous interest due their numerous applications in industrial and geophysical processes. Despite this, the behaviour of particle flows remains not totally understood and a general constitutive law to represent its behaviour has remained elusive. A crucial advance to elucidate this issue was to establish the inertial rheology for the case of quasi-rigid particles flowing steadily in a simple shear cell [1–3]. In this case it is possible to form just one dimensionless parameter called the 'inertial number' $I = d|\dot{\gamma}|/\sqrt{p/\rho_p}$, where d represents the mean diameter of the particles, $\dot{\gamma}$ corresponds to the shear rate, p is the confining pressure exerted by the walls, and ρ_p is the mass density of the particles. Hence, output variables like the effective friction coefficient $\mu = |\sigma_{xy}|/p$, where σ_{xy} represents the shear component of the stress tensor $\boldsymbol{\sigma}$, as well as the packing fraction ϕ, are sole functions of the inertial number, that is: $\mu(I)$ and $\phi(I)$.

Dense particle flows occur for $I \leq 0.1$, while quasi-static flows are commonly assumed at $I \leq 10^{-4}$ [4]. The dense flows which are not quasi-static correspond to the inertial regime where the rheology $\mu = \mu(I)$ was obtained. This inertial rheology and its extension to 3D (see [5]) have been intensively tested in steady state conditions. The test results show that the inertial rheology is not always satisfied for inhomogeneous fields at low or moderate shear rate where non-local effects cannot be neglected [6–8]. The 3D extension to the inertial rheology, which assumes that stress and shear rate tensors remain aligned, is also not satisfied for some cases like rotating drums, but still the invariants of these two tensors are generally related well via the $\mu(I)$ relation in regions of faster flow [9].

On the other hand, transient processes for granular flows are not within the purview of these steady rheological models. There is a general agreement that the granular microstructure is important for modeling transient processes. While elasto-plastic and elasto-visco-plastic models have

This article is part of the Topical Collection: In Memoriam of Robert P. Behringer.

✉ Ken Kamrin
kkamrin@mit.edu

Eduardo Rojas Parra
eduardo.rojas@uantof.cl

[1] Department of Mechanical Engineering, University of Antofagasta, Antofagasta, Chile

[2] Department of Mechanical Engineering, Massachusetts Institute of Technology, Cambridge, USA

Published online: 27 August 2019

been adapted to introduce microstructure [10, 11], there are some models that add a new and independent equation. These equations have been formulated in an incremental form for a so-called *anisotropy modulus* scalar variable as in [12, 13], and also, in a differential form applied to the fabric tensor as in [14–18].

In this study, a general continuum model is presented for unsteady shear processes in a dense granular medium. The model assumes that during transients, the granular structure, represented by the fabric tensor, changes according a differential evolution equation. Also, we establish a relationship between the stresses, specifically the effective friction coefficient μ, and the structure. We have rooted our work in relationships obtained previously in [15]. Important changes were made to obtain improved accuracy, and we have applied stringent shear reversal tests as part of our validation to achieve better qualitative and quantitative agreement between continuum and discrete simulations.

2 Numerical set-up

The numerical experiment consists of a two-dimensional dry granular medium confined between two rough walls in the absence of gravity (see Fig. 1a). The medium is made of a polydisperse mixture of circular grains with uniform mass density and diameters that are uniformly distributed in the range $[0.5d, 1.5d]$, where d is the average diameter. This distribution allows the system to have stable mixtures that do not present segregation or crystallization. The walls are made of particles of diameter d, which are forced to move at imposed velocities $\pm U_w$ to produce a Couette flow. The pressure p on the walls is controlled in order to keep it constant during the transient process. The height of the system is $H = 37d$ while the base width is $W = 4H$.

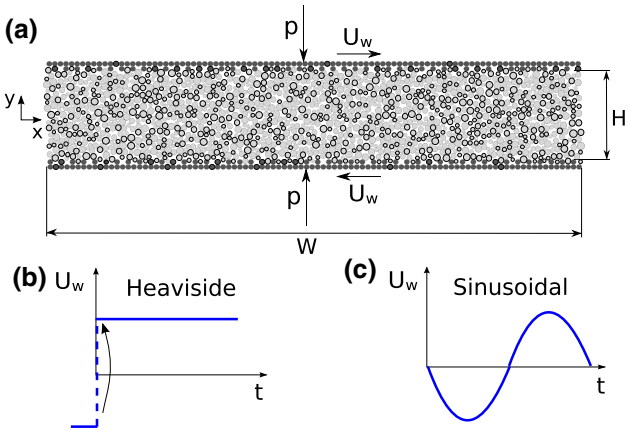

Fig. 1 **a** Numerical set-up. The height of the system is $H = 37d$ while the base width is $W = 4H$. The imposed wall velocities are: **b** Heaviside reversal and **c** sinusoidal reversal

The transient is achieved by changing the velocity of the walls in two ways: (a) an instantaneous reversal of the velocity or Heaviside signal and (b) a sinusoidal signal (see Fig. 1b and c). Thereby we impose a shear rate in the media that is a function of time $\dot{\gamma}(t)$. The inertial number I is on the order of 10^{-4}, small enough to ensure the quasi-static regime.

The discrete element method (DEM) used in this work considers a usual contact model, where normal and tangential elastic forces are linear with elastic constants k_n and k_t, respectively. The spring constant for the normal force is set to obtain an overlap of the particles $\delta = 2 \cdot 10^{-5} d$, ensuring we remain in the hard particle limit. The tangential spring constant is fixed to $k_t = 0.5 k_n$ and the dissipative terms are fixed to obtain a restitution coefficient $e = 0.5$ for the collision between two particles of diameter d. The Coulomb friction coefficient is chosen equal to $\mu_p = 0.45$. The simulations were run using the YADE discrete element code [19].

3 Model

Below, we present a contact network dependent model for the stress ratio specialized for shear dominated flows. A generalization that includes volumetric effects is discussed briefly thereafter. The network is represented by the fabric tensor obtained from the unit contact vectors between particles. As the contact structure during the transient evolves, we also include an evolution equation for the fabric, which represents a relationship between the fabric, shear rate and spin tensors. We define the (deviatoric) fabric tensor as the symmetric traceless second order tensor:

$$\mathbf{A} = -\frac{1}{2}\mathbf{I} + \frac{1}{N_c}\sum_{c\in V} \mathbf{n}\otimes\mathbf{n}, \tag{1}$$

where $\mathbf{n}$ is the unit contact vector and N_c corresponds to the number of contacts c inside of the volume V. We denote the strain-rate tensor by $\mathbf{D} = \frac{1}{2}\left(\nabla\mathbf{v} + (\nabla\mathbf{v})^T\right)$ and the spin tensor by $\mathbf{W} = \frac{1}{2}\left(\nabla\mathbf{v} - (\nabla\mathbf{v})^T\right)$, where $\mathbf{v}$ corresponds to the velocity field. For a 2D system, the deviatoric part of the shear rate tensor is given by $\mathbf{D}' = \mathbf{D} - \frac{1}{2}\mathbf{tr}(\mathbf{D})\mathbf{I}$. In our DEM simulations the vertical gradient of the vertical velocity associated to dilation was essentially noise around zero, hence we consider: $\mathbf{D} \approx \mathbf{D}' \approx 0.5\dot{\gamma}(\hat{\mathbf{i}}\otimes\hat{\mathbf{j}} + \hat{\mathbf{j}}\otimes\hat{\mathbf{i}})$.

3.1 Friction model

We find from the molecular dynamics simulations that there is not a one-to-one relationship between the (signed) stress ratio σ_{xy}/p and the off-diagonal fabric component in

the presence of shear reversals (see Fig. 2a). Better agreement is achieved by relating $\mu = |\sigma_{xy}|/p$ with a new variable $X = \mathbf{A} : \mathbf{D}'/|\mathbf{D}'|$ (see Fig. 2b). Here, colon corresponds to the inner product defined for tensors (e.g. $\mathbf{M} : \mathbf{N} = M_{ij}N_{ij}$), and $|\cdot|$ represents tensorial modulus (e.g. $|\mathbf{M}| \equiv \sqrt{\mathbf{M} : \mathbf{M}}$). This new variable represents the part of $\mathbf{A}$ in the direction of $\mathbf{D}'$ and it is negative at steady state because these tensors are almost proportional but point in opposite directions. Also, at steady state, one of the principal directions of $\mathbf{A}$ is parallel to the average direction of contacts. In this study, we are going to consider this principal direction θ_A as the direction of $\mathbf{A}$ (measured counterclockwise respect to the x axis).

Figure 2b shows the sequence of the transient process for both Heaviside and sinusoidal strain rate reversals. Here, the yellow point represents the steady state condition before the reversal. As the inertial number tends to zero for the entire process, the steady state effective friction coefficient takes the threshold value $\mu_c = \mu(I \cong 0)$. When the strain changes its direction, the reversal occurs and the variable X becomes instantaneously positive (reversal 1). In this moment, the fabric and the shear rate tensors point for one instant in the same direction. This condition generates compression perpendicular to the force chains, starting a fast process of grain network destruction, which causes the strength to decay (trajectory 2). Finally, there is a slower process where the effective friction coefficient comes back to its steady value and the force network reaches a new steady state direction, perpendicular to the previous one (trajectory 3).

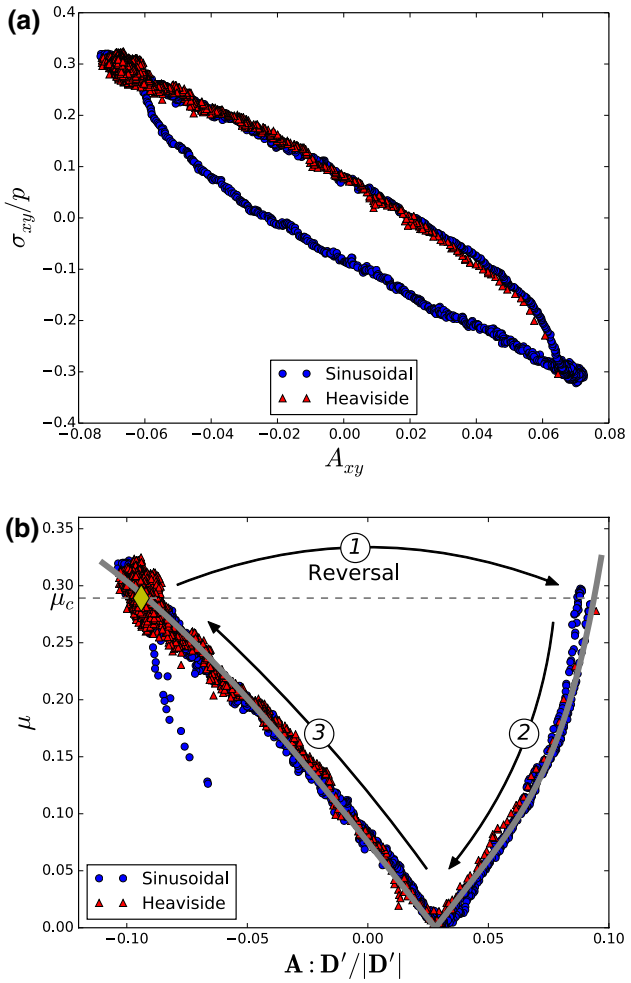

Fig. 2 Effective friction coefficient μ versus fabric (from DEM simulations). **a** Signed stress ratio σ_{xy}/p versus the xy component of the fabric tensor, A_{xy}. **b** μ versus $X = \mathbf{A} : \mathbf{D}'/|\mathbf{D}'|$. The yellow point corresponds to the steady state condition. Solid gray line represents the fit $\mu(X)$ given in Eq. (2)

The fit $\mu(X)$ for the curve shown in Fig. 2b, constitutes the model for μ written below as a function of $y(X) = X - 0.028$:

$$\mu(X) = \begin{cases} -2.7\, y(X) + 20\, y(X)^3 & , y(X) < 0 \\ 2.7\, y(X) + 9.0 \cdot 10^4\, y(X)^5 & , y(X) \geq 0. \end{cases} \tag{2}$$

The $\mu = \mu(X)$ relationship in our model replaces the quadratic form of the similar variable $\eta = a_1 + a_2 X + a_3 X^2$ from [15], where the a_i are constant values. Indeed, the variable X has some beneficial characteristics for the analysis at hand: it is dimensionless, it is independent of shear rate direction at steady state, and it is independent of shear rate magnitude.

Assuming that the deviatoric part of the stress and the strain rate are aligned, it is possible to write a generalized friction law:

$$\boldsymbol{\sigma}' = \frac{\mu(X)p}{\sqrt{2}} \frac{\mathbf{D}'}{|\mathbf{D}'|}. \tag{3}$$

The shear-specialized formulation we have presented above is not valid when the system is static or when the strain-rate deviator is otherwise null. In these cases, the shear stress $\boldsymbol{\sigma}'$ could be equal to the null tensor, but $\boldsymbol{\sigma}'$ also could be finite, given by a solid-like model such as elasticity [20, 21], which is beyond of the objectives of this work. Equation (3) would also not apply in isotropic compression/extension, where the shear stress $\boldsymbol{\sigma}'$ and the deviator of the shear rate tensor $\mathbf{D}'$ are null, but $\mathbf{D}$ is not. In this particular case, one option is to consider a modified model as in [15] where $\boldsymbol{\sigma}' = \frac{\eta p}{\sqrt{2}} \frac{\mathbf{D}'}{|\mathbf{D}|}$. The scalar variable η is related to the effective friction coefficient via the modulus of $\mathbf{D}$ and $\mathbf{D}'$, but both μ and η should be very similar in shear-dominated flow, i.e. $\eta = \mu \frac{|\mathbf{D}|}{|\mathbf{D}'|} \approx \mu$.

3.2 Fabric tensor model

We assume that the fabric tensor is governed by an independent evolution equation during the transient with the following form:

$$\overset{\triangledown}{\mathbf{A}} = \Psi(\mathbf{A}, \mathbf{D}') \equiv \alpha_1 \mathbf{D}' + \alpha_2 |\mathbf{D}'| \mathbf{A}, \tag{4}$$

where $\overset{\triangledown}{\mathbf{A}} = \dot{\mathbf{A}} + \mathbf{AW} - \mathbf{WA}$ is the *Jaumann Rate* and $\dot{\mathbf{A}}$ is the material time derivative of $\mathbf{A}$. The Jaumann or co-rotational rate, in contrast with the material time derivative, is a frame-indifferent tensorial rate, which vanishes for all rigid-body motions of the material. The function for Ψ shown above on the right-hand side was arrived at by first applying a well-known representation theorem for symmetric tensors [22], which limits the possible ways Ψ can depend on its inputs. We then keep only the lowest order terms in this expansion and, in accord with the representation theorem, allow the scalar prefactors for each term to depend only on joint scalar invariants of $\mathbf{A}$ and $\mathbf{D}'$. By expressing those prefactors as α_1 and $\alpha_2|\mathbf{D}'|$, as shown above, where the $\alpha_{1,2}$ are functions of only rate-independent invariants, the entire evolution model is assured to be rate independent.

In general, the first term on the right side of Eq. (4) pushes the fabric to grow in the direction of principal compression of the flow, while the second one opposes its growth and eventually stops the fabric evolution under continual shearing, admitting a steady fabric state. In this equation, if the coefficients α_i are chosen as $\alpha_1 = c_1$ and $\alpha_2 = c_2 + c_3(\mathbf{A} : \mathbf{D}')/|\mathbf{D}|$, where c_i are constant values, and if we consider that $|\mathbf{D}|$ is approximately $|\mathbf{D}'|$ in our shear flows, we would arrive at the same equation in [15] for the fabric deviator, i.e.

$$\overset{\triangledown}{\mathbf{A}} = c_1\mathbf{D}' + c_2|\mathbf{D}|\mathbf{A} + c_3(\mathbf{A} : \mathbf{D}')\mathbf{A}. \tag{5}$$

Using the information available from DEM simulations, we solved Eq. (4) considering the coefficients α_i as unknowns for two kinds of shear reversal: Heaviside and sinusoidal. It was found that the coefficients of the evolution equation are not constants but are rather well-represented as a single function of the new variable $X = \mathbf{A} : \mathbf{D}'/|\mathbf{D}'|$, noting that X is a valid, joint scalar invariant of $\mathbf{A}$ and $\mathbf{D}'$. Figure 3 shows two regions where the coefficients α_i behave in a different way. The right side of region B represents the beginning of the reversal, while region A represents a zone near the steady state (points where $X < -0.05$ were omitted because of the noise of the results in this zone). In region A, α_1 was fitted as a negative constant value, while α_2 was fitted as a linear function of X. Region B is noisy but the coefficients clearly show a strong tendency to decrease for α_1 and increase for α_2 until point $X_0 = 0.0827$, where both coefficients diverge. The fit functions we choose for α_i are:

$$\alpha_i = \begin{cases} a_i + b_i X & , X \leq 0 \\ a_i + b_i X + c_i \frac{X^{d_i}}{X - X_0} & , X > 0, \end{cases} \tag{6}$$

where the constant parameters involved are shown in Table 1. Note the function is continuous and differentiable at $X = 0$. Figure 3 also shows the best fits found for the evolution model given in [15] (see Eq. 5).

Table 1 Fitting parameters for the coefficients α_i of the Eq. (6)

i	a_i	b_i	c_i	d_i
1	−1.8	0	21	1.5
2	−9.0	100	−900	2.0

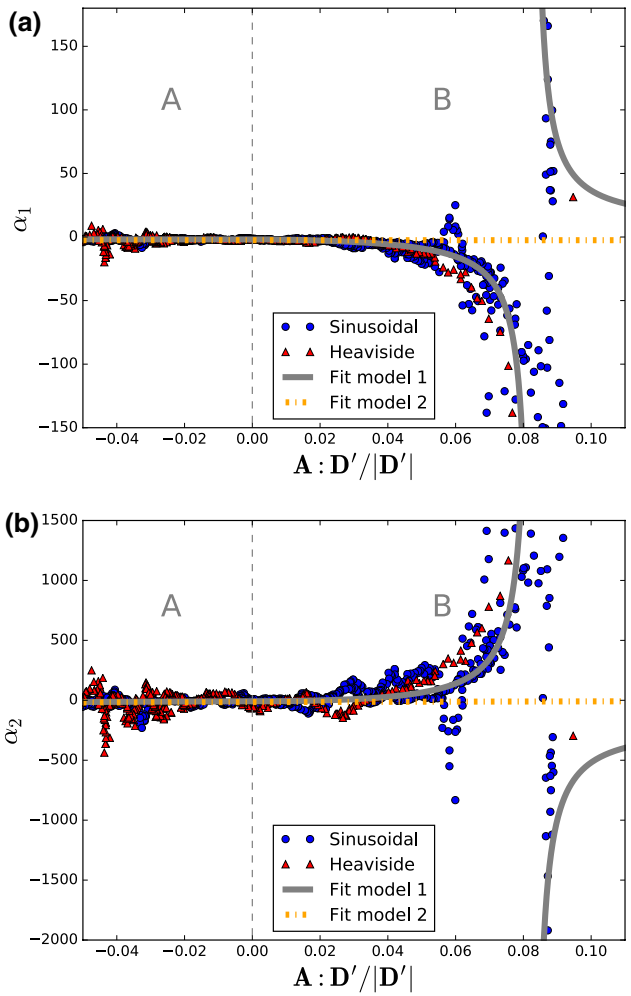

Fig. 3 Coefficients α_i obtained from Eq. (4). Solid gray line represents the fit considered in this work (Model 1), while dashed orange line represents the model given in [15] (Model 2). **a** α_1 versus $X = \mathbf{A} : \mathbf{D}'/|\mathbf{D}'|$. **b** α_2 versus $X = \mathbf{A} : \mathbf{D}'/|\mathbf{D}'|$

4 Results

We solved the fabric evolution equation numerically for the model presented in this work (Model 1) and for the previous one given in [15] (Model 2), by using the fourth-order Runge-Kutta method. For both cases, Eq. (2) was used to obtain the shear stress ratio μ. We express the fabric tensor

in terms of its modulus $|\mathbf{A}|$ and the angle of its major principal vector $\theta_{\mathbf{A}}$, which corresponds approximately to the compression direction of the force chains.

Figures 4 and 5 show the results for the fabric tensor models and the effective friction coefficient μ, in comparison with DEM simulations, for an imposed Heaviside and sinusoidal reversal, respectively. Both Model 1 and 2 present a good agreement with DEM simulation for $|\mathbf{A}|$. However, in general Model 1 captures more accurately the very strong fall just after the reversal. The transient of the fabric angle is not captured for the previous model and turns in the opposite direction in some cases. Instead, the data shows the fabric angle always passes through a vertical orientation, which the new model captures and it is attributed to the more robust fit of the coefficients α_i when the variable X is in zone B of Fig. 3. The sinusoidal shear test shows that the width of the transition in θ_A during reversal is too sharp in Model 2, and is closer to the data in the new model. Finally, the correlation presented in Eq. 2 for μ shows the new model does a better job at the beginning of the reversal process where the change in μ happens very quickly (see zoom-in inserted in Fig 4c).

5 Conclusion

In this paper, the rheology for unsteady dry granular flows in a Couette cell is studied in the quasi-static limit. We find that the rheology in this case depends on the structure of the granular medium represented by the fabric tensor, $\mathbf{A}$. We also find that the effective friction coefficient μ is a one-to-one function of the fabric tensor contracted with the shear rate tensor direction, $X = \mathbf{A} : \mathbf{D}'/|\mathbf{D}'|$.

We have presented an improved evolution equation to predict the fabric tensor behaviour and friction evolution during the transient, including coefficients that depend on the structure through the variable X. This offers certain improvements over a previous model proposed in [15]. The model is capable of capturing the abrupt fall in the fabric modulus and in the effective friction coefficient just after flow reversal, when the network is destroyed and the medium becomes almost isotropic. During this starting lapse of time, the angle of the fabric changes its direction to the opposite steady-state value in a soft way. This behaviour is well predicted by our non-constant coefficient model. Aside from predicting the effective friction, our improvement to the fabric evolution could be useful in problems where the network orientation plays a direct role in some physical phenomenon, e.g. in determining macroscopic conductivity in flowing granular systems of conductive particles, or in predicting anisotropic passage of pressure waves. However, the new fabric model is very sensitive to small changes in the coefficients. This

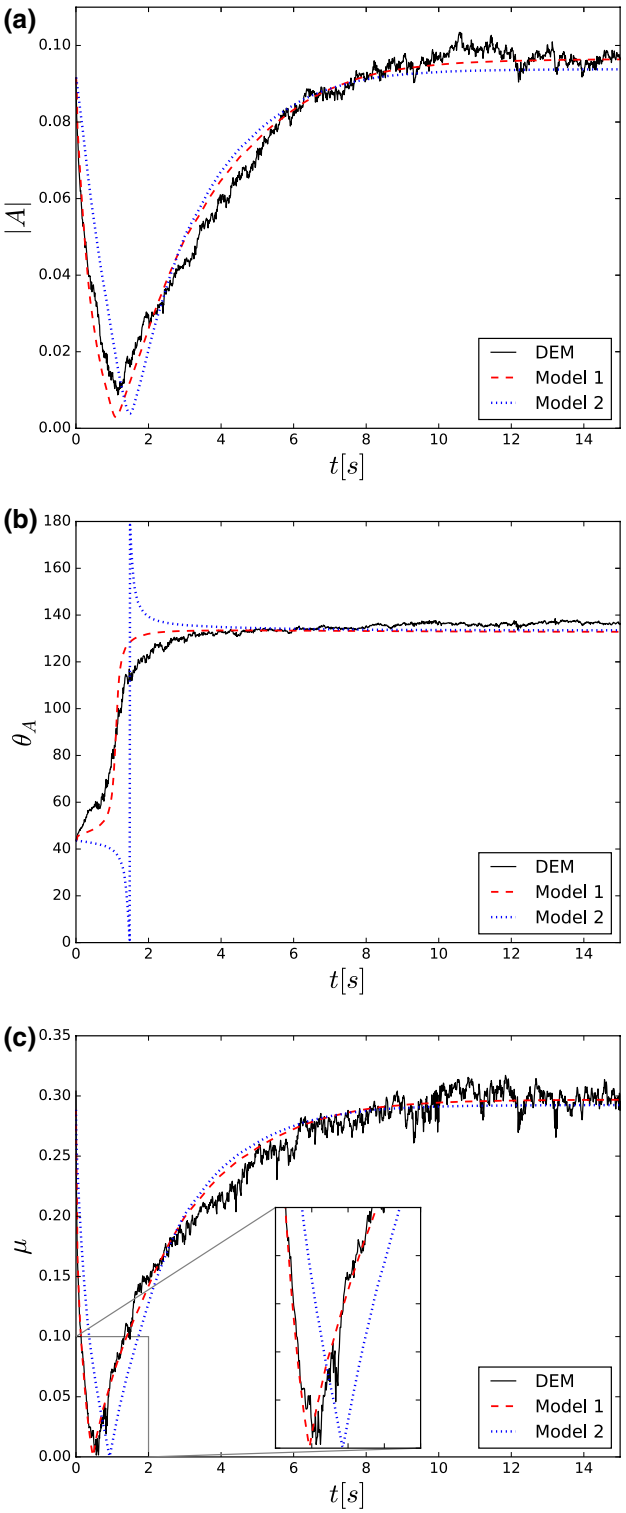

Fig. 4 Results for the Heaviside reversal case. Solid black line represents DEM simulation results, dashed red line results obtained using the model developed in this work (Model 1), while dotted blue line results obtained using the model given in [15] (Model 2) (color figure online)

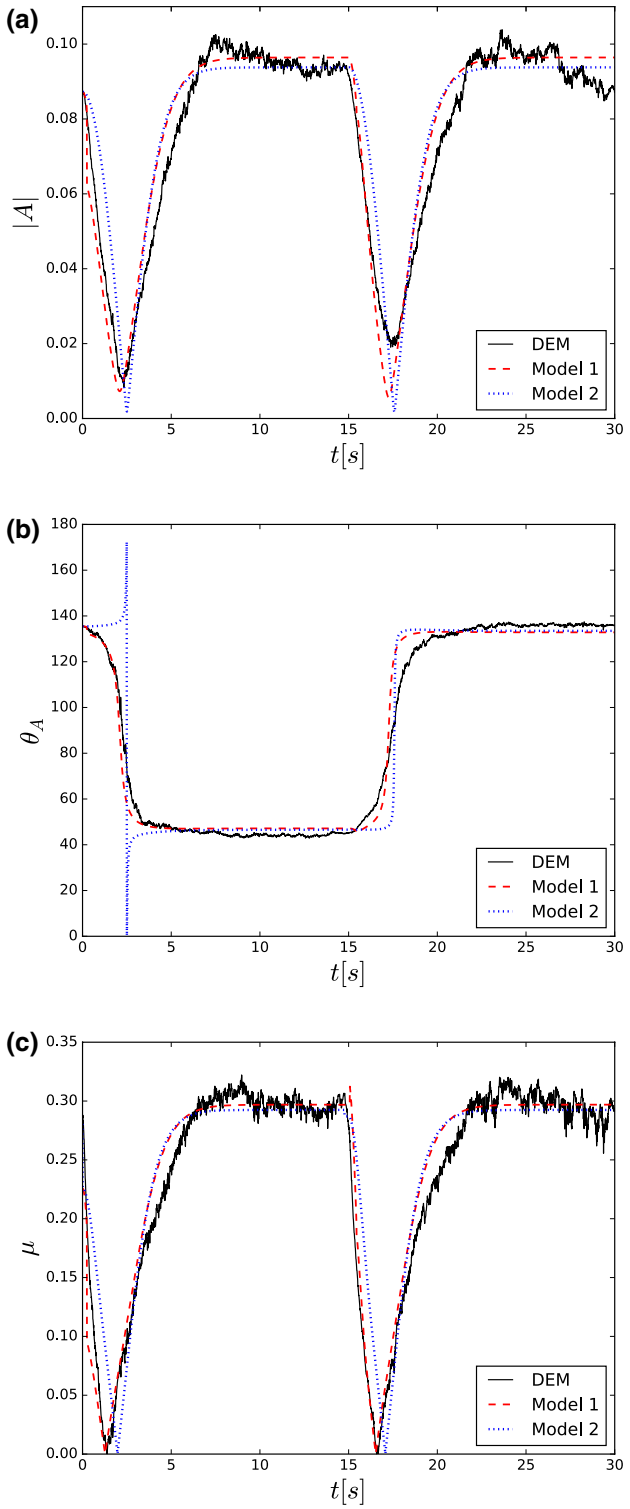

Fig. 5 Results for the sinusoidal reversal case. Solid black line represents DEM simulation results, dashed red line results obtained using the model developed in this work (Model 1), while dotted blue line results obtained using the model given in [15] (Model 2) (color figure online)

could be related to the fact that the coefficients diverge at $X = X_0$, necessitating high accuracy numerical integration.

Acknowledgements ER would like to acknowledge support from Comisión Nacional de Investigación Cientıfica y Tecnológica. KK acknowledges support from NSF Grant CBET-1706193.

Compliance with ethical standards

Conflict of interest The authors declare that they have no conflict of interest.

References

1. MiDi, G.D.R.: On dense granular flows. Eur. Phys. J. E **14**(4), 341–365 (2004)
2. Jop, P., Forterre, Y., Pouliquen, O.: A constitutive law for dense granular flows. Nature (London). **441**, 727 (2006)
3. Da Cruz, F., Emam, S., Prochnow, M., Roux, J.N., Chevoir, F.: Rheophysics of dense granular materials: discrete simulation of plane shear flows. Phys. Rev. E **72**(2), 021309 (2005)
4. DeGiuli, E., McElwaine, J.N., Wyart, M.: Phase diagram for inertial granular flows. Phys. Rev. E **94**(1), 012904 (2016)
5. Jop, P.: Hydrodynamic modeling of granular flows in a modified Couette cell. Phys. Rev. E **77**(3), 032301 (2008)
6. Aranson, I.S., Tsimring, L.S., Malloggi, F., Clément, E.: Nonlocal rheological properties of granular flows near a jamming limit. Phys. Rev. E **78**(3), 031303 (2008)
7. Kamrin, K., Koval, G.: Nonlocal constitutive relation for steady granular flow. Phys. Rev. Lett. **108**(17), 178301 (2012)
8. Bouzid, M., Trulsson, M., Claudin, P., Clément, E., Andreotti, B.: Nonlocal rheology of granular flows across yield conditions. Phys. Rev. Lett. **111**(23), 238301 (2013)
9. Cortet, P.P., Bonamy, D., Daviaud, F., Dauchot, O., Dubrulle, B., Renouf, M.: Relevance of visco-plastic theory in a multi-directional inhomogeneous granular flow. EPL (Europhys. Lett.) **88**(1), 14001 (2009)
10. Einav, I.: The unification of hypo-plastic and elasto-plastic theories. Int. J. Solids Struct. **49**(11–12), 1305–1315 (2012)
11. Babeyko, A.Y., Sobolev, S.V.: High-resolution numerical modeling of stress distribution in visco-elasto-plastic subducting slabs. Lithos **103**(1–2), 205–216 (2008)
12. Luding, S., Perdahcıoğlu, E.S.: A local constitutive model with anisotropy for various homogeneous 2D biaxial deformation modes. Chem. Ing. Tech. **83**(5), 672–688 (2011)
13. Kumar, N., Imole, O.I., Magnanimo, V., Luding, S.: Effects of polydispersity on the micro-macro behavior of granular assemblies under different deformation paths. Particuology **12**, 64–79 (2014)
14. Goddard, J.D.: A dissipative anisotropic fluid model for non-colloidal particle dispersions. J. Fluid Mech. **568**, 1–17 (2006)
15. Sun, J., Sundaresan, S.: A constitutive model with microstructure evolution for flow of rate-independent granular materials. J. Fluid Mech. **682**, 590–616 (2011)
16. Zhu, H., Mehrabadi, M.M., Massoudi, M.: Incorporating the effects of fabric in the dilatant double shearing model for planar deformation of granular materials. Int. J Plast. **22**(4), 628–653 (2006)
17. Sun, J., Sundaresan, S.: Radial hopper flow prediction using a constitutive model with microstructure evolution. Powder Technol. **242**, 81–85 (2013)

18. Olsen, T., Helal, A., McKinley, G.H., Kamrin, K.: Coupled dynamics of flow, microstructure, and conductivity in sheared suspensions. Soft Matter **12**(36), 7688–7697 (2016)
19. Šmilauer, et al.: Yade Documentation, 2nd edn. The Yade Project (2015). https://doi.org/10.5281/zenodo.34073. http://yade-dem.org/doc/
20. Kamrin, K.: Nonlinear elasto-plastic model for dense granular flow. Int. J. Plast. **26**(2), 167–88 (2010)
21. Dunatunga, S., Kamrin, K.: Continuum modelling and simulation of granular flows through their many phases. J. Fluid Mech. **779**, 483–513 (2015)
22. Rivlin, R.S.: Further remarks on the stress-deformation relations for isotropic materials. J. Ration. Mech. Anal. **4**(5), 681–702 (1955)